Available online at www.sciencedirect.com
SCIENCE DIRECT
Journal of Photochemistry and Photobiology A: Chemistry 181 (2006) 297–305
Journal of Photochemistry and Photobiology A:Chemistry
www.elsevier.com/locate/jphotochem

An acrylate polymerisation initiated by iron doped titanium dioxide

C. Damm *

University of Erlangen-Nuremberg, Institute of Polymer Materials, Martensstrasse 7, 91058 Erlangen, Bavaria, Germany

Received 14 June 2005; received in revised form 23 November 2005; accepted 10 December 2005
Available online 23 January 2006

Abstract

Fe^{3+} ion doped anatase samples with homogenously distributed Fe^{3+} ions within the TiO_2 particles were prepared using a sol–gel technique followed by a thermal treatment of the resulting powders.

The photocatalytic initiation of the polymerisation of an ethoxylated trisacrylate was investigated as a function of the Fe^{3+} content of TiO_2 pigment grains. The polymerisation rate slightly increases with increasing Fe^{3+} content of the TiO_2 in the concentration range from 0.1 to 1 mol% Fe^{3+}. Maximum polymerisation rate r_p^{max} is observed at 1 mol% Fe^{3+} followed by decreasing rates at increasing Fe^{3+} contents. A TiO_2 sample containing 10 mol% Fe^{3+} does not show any photocatalytic activity.

For the polymerisation the heterogeneous photocatalytic formation of initiating radicals is essential. Thus the results of the photopolymerisation experiments may be explained on the basis of the charge carrier lifetime in the surface/subsurface region and the UV–vis absorption properties of the samples: Photo-EMF investigations reveal that Fe^{3+} doping decreases the charge carrier lifetime in the surface region of TiO_2 from about 23 ms for the undoped material down to about 1.5 ms for samples containing 3 mol% or more Fe^{3+} indicating a very fast capturing of photochemically produced electrons by Fe^{3+}. For homogeneously distributed Fe^{3+} contents ranging up to 1 mol% this detrimental effect of Fe^{3+} doping may be compensated by an improvement of light absorption properties of the TiO_2 crystallites in the visible range. At higher Fe^{3+} concentrations XRD amorphous Fe_2O_3- or iron-rich TiO_2-phases are formed at the grain boundaries. These iron-rich phases act as light filters, so reducing the light absorption by the photocatalytically active TiO_2 crystallites. These amorphous phases should not show any photocatalytic activity.

Keywords: Photopolymerisation; Iron doped TiO_2; Photo-EMF

1. Introduction

The heterogeneous photocatalysis is an actual research field. First applications in the degradation of organic air and water pollutants were proposed [1–7].

Because of its good photocatalytic activity, high photostability and no toxicity the anatase polymorph of TiO_2 is the mostly used photocatalyst material. One disadvantage of this material is its high band gap energy of 3.2 eV [8]. This means the long wavelength absorption edge of TiO_2 amounts to about 390 nm. So the whole visible light spectrum cannot be exploited confining the efficiency of heterogeneous photocatalytic reactions. Much effort was done to overcome this problem. One way to do this may be a spectral sensitisation of TiO_2 by dyes like perylene derivatives [9], phthalocyanines [9–11], porphyrines [12] or Ru(II)-complexes [8,13,14]. But the long-term stability of sensitised TiO_2 photocatalysts may be limited by self degradation of the sensitising dyes on the catalyst surface. Moreover the dyes cover partially the TiO_2 surface lowering the photoactivity in the UV range by light absorption.

For that reason doping TiO_2 by coloured transition metal ions may be a good alternative to dye sensitisation. A plenty of papers deal with doping effects on the photocatalytic activity of TiO_2. Some important examples should be discussed here: in [15] it was shown that doping TiO_2 by metal ions with a valence higher than 4+ increases the photoactivity of TiO_2. Contrary to that finding in [16] was reported that doping TiO_2 by metal ions with a valence of 3+ or 5+ has a detrimental effect on the photocatalytic activity of TiO_2. A systematic study of doping effects was performed using 21 different metal ions [17]. There could be shown that the energy level and the d-electron configuration of the metal ions govern the activity of TiO_2.

Possible sensitisation effects of coloured metal ions were not discussed.

* Tel.: +49 9131 85 27748; fax: +49 9131 85 28321.
E-mail address: Cornelia.damm@ww.uni-erlangen.de.

1010-6030/$ – see front matter © 2005 Elsevier B.V. All rights reserved.
doi:10.1016/j.jphotochem.2005.12.011

Often the results are controversial showing that the influence of metal ions on the photocatalytic activity of TiO_2 is not well understood in detail.

An important feature is the distribution of the dopant within the TiO_2 grains.

One reason for the poor reproducibility of the results may cause from differences in the distribution of dopings due to different preparation methods. In [18] it was shown that doping only the inner part of TiO_2 particles by Mo^{6+} enhances its photocatalytic activity. A homogenous distribution of Mo^{6+} or a surface doping lowers the activity of TiO_2 [18]. The results are explained on the basis of heterojunctions favouring a separation of electron/hole pairs. But the synergistic and antagonistic effects are not understood completely.

An investigation of the photoelectric properties of the catalyst materials in combination with photocatalytic activity tests may be a valuable tool to get a better understanding of doping effects. But only a few researchers combine photocatalytic investigations with Photo-EMF measurements using the same photocatalyst material [19,20,21]. In [19,20] it was shown that doping TiO_2 by Mo^{5+}, Cr^{3+} or Fe^{3+} leads to a strong decrease of the charge carrier lifetime in the surface region because the dopants occupy lattice places and act there as recombination centres. This finding can explain the detrimental effect of these dopants on the photocatalytic activity of TiO_2 observed in [19,20]. On the other hand it may be expected that an inhomogeneous distribution of dopants can create heterojunctions which may favour the charge separation.

The goal of this work is the investigation of the influence of doping TiO_2 by Fe^{3+} ions on its photoelectric properties and on the photocatalytic activity. The photopolymerisation of an ethoxylated trisacrylate is used as a test reaction to check the photocatalytic activity because up to now little is known about heterogen photocatalytic polymerisations [21–26]. The efficiency of heterogeneous photocatalytic reactions mostly is rather low. For that reason reaction times of some hours are often necessary to observe the kinetics of heterogeneous photocatalytic reactions. In the case of polymerisations the photocatalytic initiation effect is amplified by the subsequent chain growth. Thus a photocatalytic initiated polymerisation reaction proceeds during minutes making such a reaction to a high throughput method for checking the activity of photocatalyst materials.

Photo-EMF measurements are used to investigate the photoelectric primary processes in the photocatalyst materials. This method was chosen because the mechanisms of Photo-EMF generation and of the formation of charge carriers in the heterogenous photocatalysis are the same.

To perform Photo-EMF measurements the sample is brought into a capacitor. A laser flash (pulse duration 300 ps) illuminates the sample through a transparent NESA glass electrode. Due to the laser impulse at the surface of the sample electrons (e^-) are excited from the valence band (VB) into the conduction band (CB) creating electron/hole pairs. According to the absorption coefficient of the actinic light both charge carriers move into the bulk of photoconductor along the direction of incident light driven by their concentration gradient. A charge separation takes place at phase boundaries, structural defects and at chemical impurity or dopant sites if the electrons and holes have different mobilities. Titanium dioxide behaves like an n-type photoconductor. This means that the mobility of electrons is higher than that of the holes. As a result mainly electrons will reach the bulk of the pigment. The spatial charge separation creates a photo-induced potential which can be measured as Photo-electromotive force (Photo-EMF).

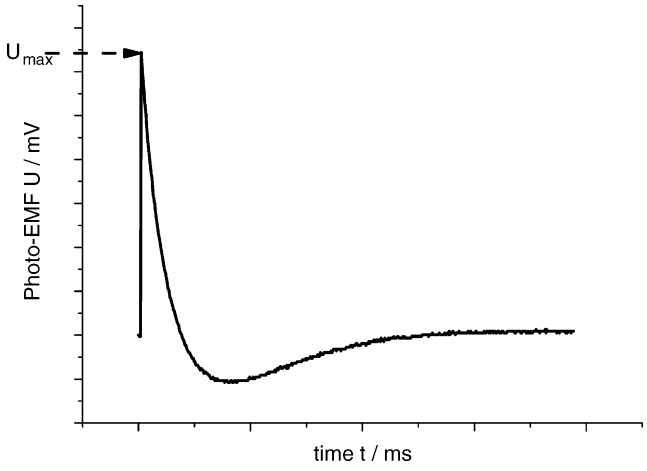

Fig. 1. Shape of the Photo-EMF signals of the investigated TiO_2 samples.

This transient photovoltage is measured contactless and without any external electric field as a function of the time. For that reason the charge carrier concentration gradient due to the gradient of light absorption and heterojunctions within the sample are the only driving forces for the Photo-EMF generation. So this method is well suited for investigations concerning the influence of materials structures on their photoelectric properties [27].

The samples investigated in this work show Photo-EMF signals as shown in Fig. 1.

The Photo-EMF signals of the samples investigated start with a positive sign and show a zero potential passage, see Fig. 1. Such signals are typical for n-type photoconductors.

The amount of the maximum Photo-EMF U_{max} upon illumination is a measure of the efficiency of charge generation and separation in competition to deactivation processes due to recombination or chemical reactions of the charge carriers. For the description of the Photo-EMF decay a biexponential rate law is used:

$$U(t) = U_1^0 \exp(-k_1 t) + U_2^0 \exp(-k_2 t) \quad (1)$$

As per definition the process with the parameters U_1^0 and k_1 always is the faster decay process. That means $k_1 > k_2$.

The cause of the biexponential decay behaviour of the Photo-EMF is a generation of two partial Photo-EMFs decaying independently. The partial voltages U_1^0 and U_2^0 are the values of both Photo-EMFs at the beginning of their decay process with k_1 and k_2 as their first order decay constants. The sum of U_1^0 and U_2^0 is U_{max}.

In a previous work was shown that a generation of a Photo-EMF in the subsurface region additional to the DEMBER-EMF

in the bulk causes the biexponential Photo-EMF decay. Usually the trap concentration in the surface and subsurface regions are higher than in the bulk resulting in band bendings near the subsurface region. So additional to the DEMBER Photo-EMF in the bulk a second one is generated in the surface/subsurface region due to band bendings. If both Photo-EMFs are opposite directed the sum of them may show a zero potential passage. That means the biexponential Photo-EMF decay is a property of pure photoconductors. According to the findings of our previous works we are able to assign the faster decay process (parameters U_1^0, k_1) to a Photo-EMF in the subsurface region of the catalyst particles [27,28]. That means U_1^0 represents a charge carrier amount in the subsurface region, k_1 is a measure of the recombination rate in the surface/subsurface region. So the charge carrier lifetime in the surface region τ_{CC} which is essential for heterogeneous photocatalysis can be derived from k_1: $\tau_{CC} = 1/k_1$.

In [28] the Photo-EMF method is described more in detail.

2. Experimental

2.1. Materials

Titanium-tetraisopropoxide, dichlormaleic acid anhydride, $Fe(NO_3)_3{\cdot}9H_2O$, ethyl acetoacetate, methanol and 1,2-dichlorethane were purchased from Merck Co., Darmstadt.

The titanium-tetraisopropoxide has a purity higher than 98%, the main impurity is *iso*-propanol. The methanol has a purity higher than 99.5% and contains water as impurity.

According to the supplier the $Fe(NO_3)_3{\cdot}9H_2O$ contains up to 0.0005 wt.% Cl^-, up to 0.005 wt.% PO_4^{3-}, up to 0.005 wt.% SO_4^{2-}, up to 0.005 wt.% Ca^{2+}, up to 0.005 wt.% Cu^{2+}, up to 0.005 wt.% K^+, up to 0.001 wt.% Mg^{2+}, up to 0.02 wt.% Mn^{2+}, up to 0.005 wt.% Na^+, up to 0.001 wt.% Pb^{2+} and up to 0.001 wt.% Zn^{2+}.

The polyvinyl butyrale used as matrix for the Photo-EMF measurements was produced by Wacker Burghausen. All materials were used as received without further purification.

The trisacrylate monomer used was purchased from Cray Valley and contains hydroquinone monomethyl ether as stabiliser. Before use the stabiliser was removed by filtration over Al_2O_3.

2.2. Preparation of the TiO_2 samples

The preparation procedure was similar to that described in [19].

The TiO_2 samples were prepared by acidic hydrolysis of a 0.01 M solution of titanium-tetraisopropoxide in methanol containing the required amount of $Fe(NO_3)_3{\cdot}9H_2O$. A 0.01 M solution of ethyl acetoacetate in methanol was used as stabiliser. The mixture was stirred 24 h at room temperature. It did not become turbid during this time. After evaporating the solvent an amorphous TiO_2 powder was received. The powder was dried at 110 °C/3 h. To produce the photocatalytic active anatase polymorph the TiO_2 samples were annealed at 450 °C/24 h in air using a muffle furnace.

2.3. Scanning electron microscopy (SEM)

The morphology of the TiO_2 samples was investigated by scanning electron microscopy (SEM) using a LEO 430 (Zeiss, Leica). For SEM investigations, gold was deposited on the powder samples.

2.4. Specific surface area

The specific surface area of the TiO_2 powders was determined by N_2 adsorption at 77 K (BET method) using a high speed gas sorption analyzer (Quantachrome). The BET specific surfaces were used to calculate the average particle sizes assuming the existence of spherical particles with a monomodal size distribution.

2.5. X-ray diffraction

Powder X-ray diffraction (XRD) was used to check the crystal structure as well as to determine the sizes of the primary crystallites. The X-ray diffraction patterns were recorded in the range of 2Θ between 20° and 70° using Cu $K\alpha_1$ irradiation (X'Pert Pro MPD, Philips).

2.6. Diffuse reflection spectroscopy

Diffuse reflection spectra were recorded on pressed powders in the wavelength range between 200 and 800 nm using an UV-2401 PC (Shimadzu). $BaSO_4$ was used as a white standard. From the reflection spectra the absorption was calculated by the Kubelka–Munk method.

2.7. Photo-EMF measurements

Photo-EMF measurements were performed using pigment polymer dispersion layers. To prepare samples for the Photo-EMF measurements, 100 mg of TiO_2 were dispersed in 3 g of a solution of polyvinyl butyrale in 1,2-dichlorethane (10 wt.%) using a one ball vibrating mill.[1] The mixture was placed on a glass slide (area: 47.6 cm^2) and dried in a solvent atmosphere. After 48 h the layer was removed from the glass and dried for 8 h in vacuum at room temperature before use.

The layers had a thickness of about 60–80 μm and a total absorption in the UV range.

Pieces having a diameter of 10 mm were cut from the layers and brought into the Photo-EMF device.

The sample was illuminated by a single flash of a nitrogen laser PNL 100; *Lasertechnik Berlin* GmbH (wavelength: 337 nm, pulse duration: 300 ps, power: 100 kW). The energy of the actinic light pulse was about 3×10^{13} quanta per flash at the sample's place. The temperature of the sample and the amplifier was 25 °C.

All Photo-EMF signals and parameters presented here are the mean values of three measurements. Each measurement was performed using a new piece of the sample.

[1] Processing conditions: 30 min milling at room temperature.

The Photo-EMF device is constructed like a capacitor with a transparent NESA glass as measuring electrode and a grounded metal plate on the rear side of the sample. The transient Photo-EMF is measured contactless using insulating foils between the sample and the electrodes. No external electric field is applied. For more details see [28].

2.8. Photopolymerisation

The light induced polymerisation of the trisacrylate (**1**) is used to investigate the photocatalytic activity of the TiO_2 samples. 6.5 mol% related to monomer of the added electron acceptor dichloromaleic acid anhydride (**2**) will provide an electron/hole symmetry over a long period of the photocatalytic initiation reaction.

The samples contained 5.5 wt.% of the respective TiO_2 powder under investigation. For comparison the mixture was also irradiated without any added TiO_2 catalyst (see dotted lines Fig. 4a and b).

To disperse the TiO_2 powder in the monomer the same milling procedure as described in Section 2.7 was used.

The polymerisation experiments were performed using a film of the pigment–monomer mixture, $d = 20\ \mu m$, and cast with a knifecoater.

The layers were illuminated with white light of a 100-W mercury high pressure lamp with an intensity of 90 mW/cm^2 at the sample's place. To avoid a direct excitation of the acrylate monomer all radiation below 350 nm was removed using a cut-off glass filter (Schott).

The relative concentration of double bonds was determined by real time infrared spectroscopy RT-FTIR with a spectrometer "FTS6000" (Biorad) monitoring the absorption band at 810 cm^{-1} (C=C–H wagging vibration) of the acrylate monomer as a function of the illumination time.

To exclude oxygen the sample chamber of the spectrometer was flushed with nitrogen 3 min before as well as during the whole irradiation time.

The results of all polymerisation experiments presented here are mean values of three attempts.

3. Results and discussion

3.1. Morphology of the TiO_2 samples

Figs. 2a and b and 3a and b, respectively, show the morphology of an undoped TiO_2 powder and a TiO_2 powder doped by 10 mol% Fe^{3+}, respectively. The morphology of the other doped TiO_2 samples is similar (not shown).

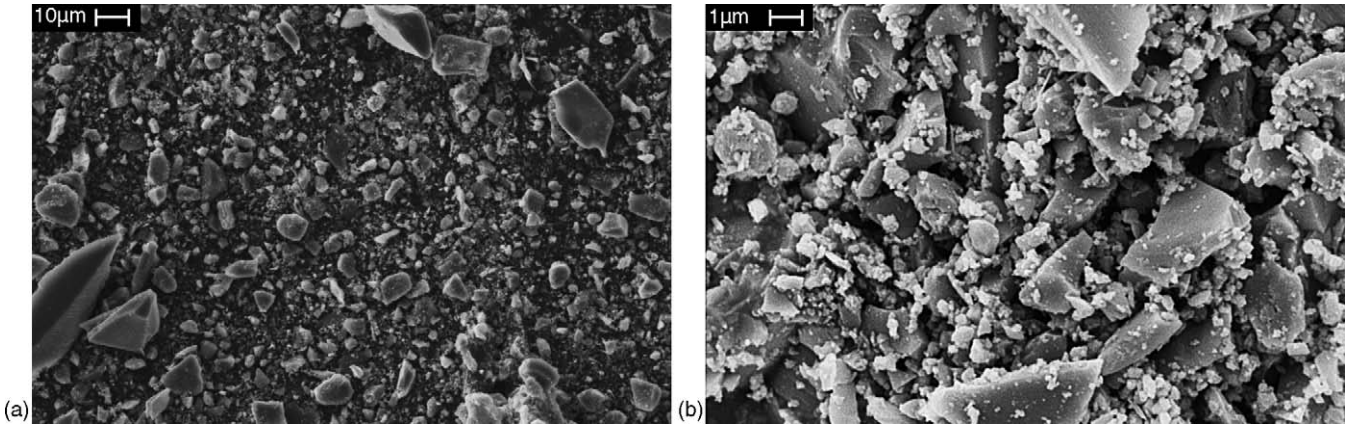

Fig. 2. SEM micrograph of an undoped TiO_2 powder sample: (a) survey, magnification 1:1000; (b) detail, magnification 1:10,000.

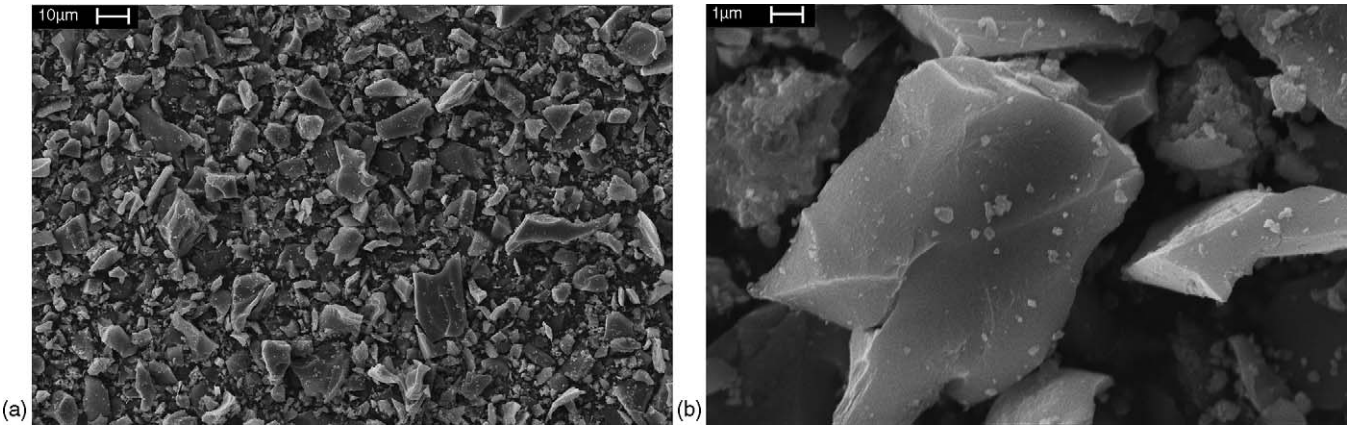

Fig. 3. SEM micrograph of a TiO_2 powder sample doped by 10 mol% Fe^{3+}: (a) survey, magnification 1:1000; (b) detail, magnification 1:10,000.

Table 1
Influence of the Fe^{3+} content in TiO_2 on the primary crystallite sizes, on the specific surface area and particle size calculated from it and on the average number of primary crystallites per particle

Fe^{3+} in TiO_2 (mol%)	Primary crystallite size (nm)	Specific surface area ($m^2\ g^{-1}$)	Particle size according to the specific surface area (μm)	No. of primary crystallites per particle
0	20	1.5	1.3	65
0.1	20	1.6	1.2	60
0.5	20	1.7	1.1	55
1	18	0.9	2.7	150
3	16	1.4	1.4	88
5	15	1.0	2.3	153
10	8	0.6	6.0	750

According to Figs. 2a and b and 3a and b, the TiO_2 particles are irregular shaped. The doping has no noticeable influence on the particle shape. The samples contain large particles having sizes between 10 and 20 μm leading to a rather low specific surface area of the samples. Besides the large particles there are finer ones having sizes below 1 μm. The amount of small particles in the undoped sample is higher than in the doped one reflecting also in the values of specific surface areas, see Table 1.

The results of static laser light scattering experiments indicate a rather broad particle size distribution in all samples investigated: in all cases the most frequent particle size is around 10 μm. But about 5 vol.% of the particles have sizes in the range from 0.1 to 1 μm.

Any heterogeneous photocatalytic reaction is a surface process. Because the surface to bulk ratio of smaller particles is much higher than that of larger ones, it can be expected that the particles having size below 1 μm contribute strongly to the activity of the sample. In our previous work it was shown that in the presence of small TiO_2 particles a higher polymerisation rate is observed than in the presence of larger ones [30].

XRD investigations give information about the crystal structure of the samples: all samples show a diffraction peak at $2\Theta = 25.28^\circ$ which is the (1 0 1) peak of the anatase polymorph. No peak could be detected at $2\Theta = 27.45^\circ$. That means all TiO_2 samples investigated in this work do not contain any rutile polymorph.

The doped TiO_2 samples also do not show any additional XRD peak. This is true even for the sample containing 10 mol% Fe^{3+}, indicating that no detectable amounts of crystalline Fe_2O_3 or $FeTiO_3$ were formed.

This result is in agreement with the literature [19] because the preparation method used is known to form homogeneous distribution of Fe^{3+} in the TiO_2. For Fe^{3+} contents smaller than 1 mol% the Fe^{3+} ions occupy places in the Ti^{4+} lattice related to the comparable radii of Fe^{3+} and Ti^{4+} [19,29]. So no separate iron phase is formed. For Fe^{3+} contents higher than 1 mol% formation of Fe_2O_3 phases is discussed in [19].

The absorption spectra of TiO_2 samples doped by 3, 5 or 10 mol% Fe^{3+} show a shoulder around 500 nm (see Fig. 7) indicating the formation of Fe_2O_3. This finding in combination with the XRD results shows that the Fe_2O_3 phases must be amorphous or their crystallinity must be below the detection limit of XRD.

Under the assumption that the primary TiO_2 crystallites have a spherical shape, after correction the instrument broadening using single-crystal silicon as standard, from the peak width at half maximum height (FWHM) of the (1 0 1) diffraction peak the size of the primary anatase crystallites was calculated using the Scherrer equation, see Table 1. For Fe^{3+} contents below 1 mol% the primary crystallite size amounting to 20 nm is not affected by doping. That means if all Fe^{3+} ions occupy lattice places, the growth of the primary anatase crystallites is not disturbed by doping.

For iron contents higher than 1 mol% the primary crystallite size decreases with increasing iron concentration, that means it decreases with increasing amount of Fe^{3+} outside of lattice places. This finding shows that an increasing number of Fe^{3+} ions not situated at lattice places hinder the growth of the primary anatase crystallites. As a consequence TiO_2 samples containing more than 1 mol% Fe^{3+} should have more grain boundaries per particle than that with lower Fe^{3+} contents, and the internal area of grain boundaries per particle should increase with increasing content of Fe^{3+} ions. Because only 1 mol% of Fe^{3+} is soluble in the TiO_2 lattice, it can be concluded that the grain boundary regions are Fe_2O_3 phases. Because grain boundaries may influence charge separation or recombination, the photoelectric properties and hence the photocatalytic activity of the TiO_2 samples should be affected by Fe^{3+} doping.

3.2. Photopolymerisation

In photopolymerisation experiments the relative monomer concentration was recorded as a function of the illumination time. From the resulting kinetic curves the illumination time $t_{30\%}$ necessary to achieve a monomer conversion of 30% was determined. Moreover the curves were differentiated and then the maximum polymerisation rate r_p^{max} was calculated.

The results are shown in Fig. 4a and b.

The dotted lines in Fig. 4a and b visualize the polymerisation parameters r_p^{max} and $t_{30\%}$ of the acrylate without TiO_2 but in the presence of the electron acceptor and may serve as reference lines to judge if a TiO_2 sample initiates a photopolymerisation or not.

With the exception of the sample doped by 10 mol% Fe^{3+} all TiO_2 samples accelerate the polymerisation of the acrylate by their photocatalytic activity although their specific surface area is rather low. The content of Fe^{3+} ions within the TiO_2 particles

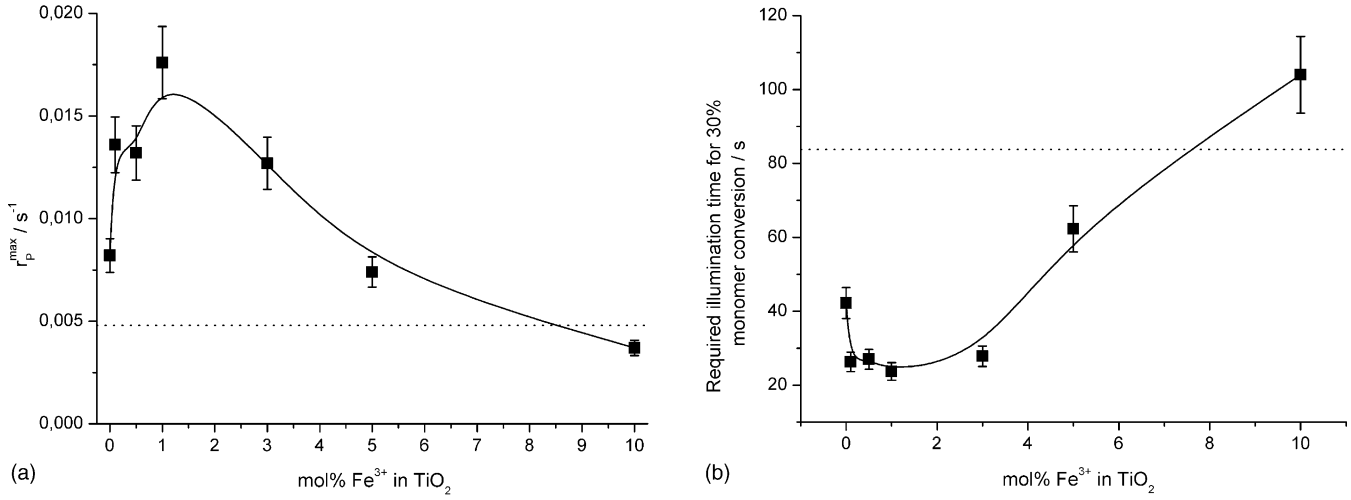

Fig. 4. (a) Influence of the Fe^{3+} content in TiO_2 on the maximum photopolymerisation rate r_p^{max} of the acrylate **1**. The dotted line visualizes the photopolymerisation rate of the acrylate without TiO_2. (b) Illumination time necessary to achieve a monomer conversion of 30% $t_{30\%}$ in dependence on the Fe^{3+} content in TiO_2. The dotted line visualizes the $t_{30\%}$ value for a reference sample without TiO_2.

affects strongly the polymerisation rate of the acrylate monomer. For Fe^{3+} contents below 1 mol% the maximum polymerisation rate increases with growing Fe^{3+} content in TiO_2. In the presence of TiO_2 containing 1 mol% Fe^{3+} the highest polymerisation rate is observed, it is more than three times higher in comparison to the reference sample without TiO_2. If the content of Fe^{3+} ions in TiO_2 is larger than 1 mol% the maximum photopolymerisation rate of the acrylate decreases with increasing Fe^{3+} content. TiO_2 containing 10 mol% Fe^{3+} is not able to accelerate the photopolymerisation of the acrylate used. This sample may act as an internal light filter. For that reason the sample containing TiO_2 doped by 10 mol% Fe^{3+} polymerises slower than the reference system.

The reaction time which is necessary to achieve a monomer conversion of 30% $t_{30\%}$ is a parameter describing an obvious conversion rate. In this parameter the polymerisation rate and the induction period are included. A small value for $t_{30\%}$ implicates a high monomer conversion rate. A monomer conversion of 30% was chosen because at this stage the viscosity increase also influencing the polymerisation kinetics is sufficient low. The total monomer conversion after illumination of 120 s was approximately 70%.

The values for $t_{30\%}$ depend on the Fe^{3+} content in TiO_2 in a similar manner like r_p^{max}, see Fig. 4b. At 1 mol% Fe^{3+} in TiO_2 $t_{30\%}$ shows a minimum, indicating maximum conversion rate. If the TiO_2 contains more than 1 mol% Fe^{3+}, then $t_{30\%}$ increases with growing content of Fe^{3+}. That means the conversion rate decreases. For the TiO_2 sample doped by 10 mol% Fe^{3+} the value of $t_{30\%}$ is even larger than that for the reference sample because this sample is not able to accelerate a photopolymerisation of the acrylate.

In [21] it was shown that the redox reaction between the illuminated photocatalyst pigment and the monomer is essential for starting a polymerisation. This was further confirmed by the finding that in the absence of the electron acceptor **2** no noticeable polymerisation of the acrylate **1** is observed because the charge symmetry in the TiO_2 is not fulfilled. Thus based on the thermodynamics of the redox processes between the illuminated (doped) TiO_2, the acrylate **1** (abbreviated as monomer M) and the electron acceptor **2** (abbreviated as A) (Fig. 5) the following mechanism of polymerisation is suggested:

- photoelectric primary processes (investigated by Photo-EMF measurements):

$$TiO_2 + h\nu\,(\lambda < 390\,\text{nm}) \rightarrow TiO_2 + e^- + h^+ \quad \text{(a)}$$

$$TiO_2/Fe^{3+} + h\nu\,(\lambda = 495\,\text{nm}) \rightarrow TiO_2/Fe^{2+} + h^+ \quad \text{(b)}$$

$$Fe^{3+} + e^- \rightarrow Fe^{2+} \quad \text{(c)}$$

- photocatalytic formation of initiating radicals:

$$M + h^+ \rightarrow M^{\bullet +} \rightarrow M^{\bullet} + H^+ \quad \text{(d)}$$

$$A + e^- \rightarrow A^{\bullet -} \quad \text{(e)}$$

$$A^{\bullet -} + H^+ \rightarrow A^{\bullet} \quad \text{(f)}$$

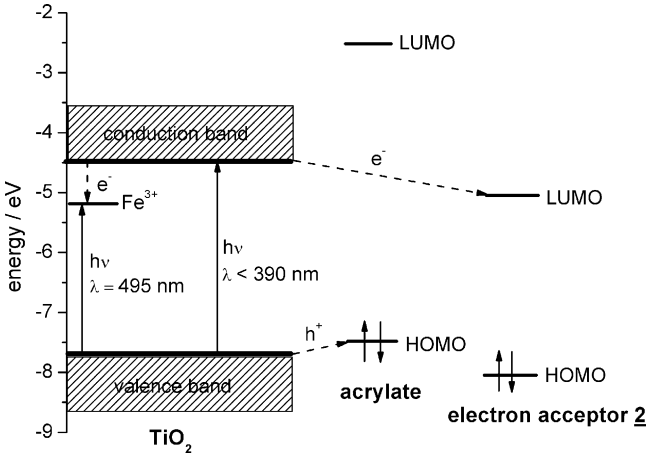

Fig. 5. Energy level diagram for the photoredox reactions between the doped TiO_2, the acrylate **1** and the electron acceptor **2** leading to a formation of initiating radical species.

- chain growth:

$$M^{\bullet} \text{ or } A^{\bullet} + nM \rightarrow (M)_n M^{\bullet} \text{ or } (M)_n A^{\bullet} \quad \text{(g)}$$

According to (a) illumination of TiO_2 with wavelengths shorter than 390 nm leads to a formation of electrons (e^-) in the conduction band and holes (h^+) in the valence band. TiO_2 doped with Fe^{3+} exploits the visible light too, leading to the production of additional h^+ in the valence band by process (b). Moreover Fe^{3+} can act as an electron trap which shortens their lifetime according to (c).

The h^+ in the valence band of TiO_2 can oxidize the monomer to a radical cation (d). The radical cation can donate a proton (H^+) to hydroxyl groups on the surface of TiO_2 leading to a formation of a monomer radical.

The TiO_2 is not able to transfer electrons (e^-) from its conduction band to the monomer. Thus for keeping charge symmetry in TiO_2 an electron acceptor is necessary. The product of the e^- transfer from the TiO_2 to the electron acceptor is a radical anion, see process (e). The radical anion can accept a proton from hydroxyl groups on the TiO_2 surface leading to a radical, see process (f). The radicals of the monomer and the electron acceptor can start the chain growth according to (g).

The chain termination occurs by radical combination or by disproportionation.

In a previous work [21] for a photocatalytic acrylate polymerisation the following rate law was found:

$$r_P = -\frac{d[M]}{dt} = k_{brutto}[M][I]^{1/2} \quad (2)$$

This rate law is accordance with the theory of radicalic polymerisations.

The chain growth rate as well as the start rate contribute to the brutto polymerisation constant $k_{brutto.}$ The chain growth rate depends on the monomer only; the start rate on the charge transfer velocity.

The monomer and its initial concentration are always the same. Thus differences in the polymerisation rate between the samples investigated are governed by different initiator concentrations [I] and different start rates. The initiator I are the radicals formed by charge transfer processes between the monomer, the electron acceptor and the photoexcited TiO_2. That means the initiator concentration increases with the photocatalytic activity of the TiO_2. If the TiO_2 would be very active, the density of radicals formed by the TiO_2 could become so high that a radical recombination would be favoured. In that case the activity of TiO_2 would not be reflected in the polymerisation rate.

However, using the methyl viologen method it was shown, that the quantum yield of radical formation of the TiO_2 samples investigated is in the range of 10^{-3}. This is about two orders of magnitude lower compared to molecular photoinitiators [31,32]. Thus under illumination molecular photoinitiators generate a higher radical concentration than heterogeneous photocatalysts. But in [33] it was shown that, if the absorbed light intensity is the same for every photoinitiator, even for molecular photoinitiators the maximum rate of an acrylate photopolymerisation increases with the square root of the quantum yield of the radical formation. The same should be true for heterogeneous photocatalytic initiators.

Moreover, an increased radical recombination caused by a high radical density should reflect in a decrease of the molecular mass of the photopolymer. But in [34] it was shown that an acrylate photopolymer prepared by heterogeneous photocatalytic polymerisation even has a higher molar mass than a photopolymer of the same monomer formed by homogenous initiation.

All these findings discussed above show that the radical density formed by the TiO_2 photocatalysts is far below the range in which an enhanced radical recombination can be expected.

3.3. Charge carrier lifetime

The rate constant k_1 of the surface Photo-EMF was calculated by fitting the measured Photo-EMF signals of the TiO_2 samples using Eq. (1). From k_1 the charge carrier lifetime in the surface region was calculated: $\tau_{CC} = 1/k_1$.

In Fig. 6 left axis the values of τ_{CC} are plotted as a function of the Fe^{3+} content in TiO_2.

The charge carrier lifetime in the surface region from undoped TiO_2 amounts to about 23 ms. Doping TiO_2 by Fe^{3+} ions lowers the charge carrier lifetime, see Fig. 6. This finding confirms the results shown in [19].

The charge carrier lifetime decreases continuously with increasing content of Fe^{3+} in TiO_2.

If the Fe^{3+} content in TiO_2 reaches 3 mol% the charge carrier lifetime decreases to a minimum value of about 1.5 ms. In TiO_2 doped by 1 mol% Fe^{3+} the charge carrier lifetime amounts about 18 ms which should be sufficient long for heterogeneous photocatalysis.

The results show that Fe^{3+} ions occupying places in the TiO_2 lattice as well as grain boundaries enhance the electron/hole recombination.

This result is opposite to findings for pure TiO_2 shown in our previous work [30]: in pure TiO_2 grain boundaries do not shorten the charge carrier lifetime but they favour the charge separation.

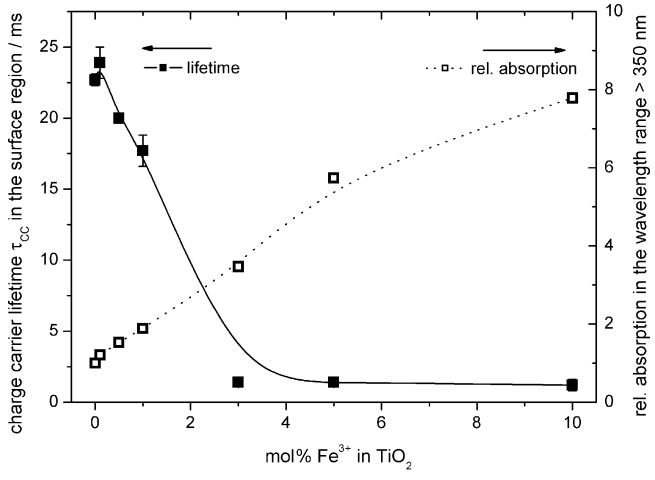

Fig. 6. Influence of the Fe^{3+} content in TiO_2 on the charge carrier lifetime τ_{CC} (left axis) and on the relative integral absorption (right axis).

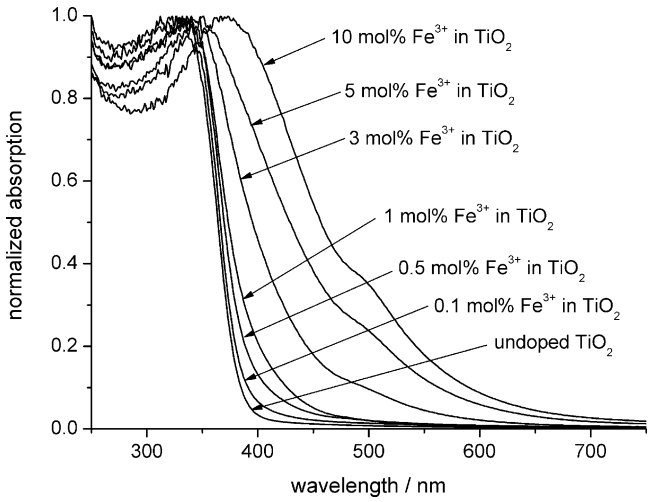

Fig. 7. Normalized absorption spectra of undoped and iron doped TiO_2 powders.

The different properties of the grain boundary regions in pure and Fe^{3+} doped TiO_2 may be explained by their compositions: in pure TiO_2 the composition in the grain boundary regions and in the crystallites should be comparable. In contrast to that in heavily Fe^{3+} doped TiO_2 Fe^{3+} ions are enriched in the grain boundary regions.

A comparison of both results shows, that grain boundaries can act as charge separation or as recombination centres. The composition of the grain boundary regions governs their properties. So only from the morphology of a catalyst material no conclusions about its photocatalytic activity can be drawn.

3.4. Light absorption properties

The absorption spectra of the TiO_2 powders calculated from their diffuse reflection spectra were normalized (Fig. 7).

The normalized spectra were integrated in the wavelength range between 350 nm and the long wavelength absorption edge of the samples. The values for the integral absorption of the doped TiO_2 samples were referred to that of the undoped one. The relative integral absorption is a qualitative measure of the improvement of the light absorption due to doping TiO_2 by Fe^{3+}.

According to Fig. 6 (right axis) the relative integral absorption increases with increasing content of Fe^{3+} ions in TiO_2. It must be taken into account that for TiO_2 samples containing more than 1 mol% of Fe^{3+} ions the iron-rich grain boundary regions contribute noticeable to the integral absorption.

4. Conclusions

The ability of TiO_2 to accelerate a photopolymerisation of the acrylate **1** by its photocatalytic activity is affected by doping by Fe^{3+} ions. Fe^{3+} concentrations between 0.1 and 3 mol% improve the photocatalytic activity of TiO_2. Larger contents of Fe^{3+} ions are detrimental. A TiO_2 sample containing 10 mol% Fe^{3+} ions does not show any photocatalytic activity.

Based on the thermodynamics of charge transfer a mechanism of the polymerisation process was suggested. The mechanism involves the formation of initiating radicals from the monomer and the electron acceptor by the photocatalytic activity of the TiO_2.

For a high photocatalytic activity a good light exploitation, an efficient charge separation and a sufficient charge carrier lifetime in the surface region of the photocatalyst material are essential preconditions.

The absorption in the wavelength range above 350 nm and with that the exploitation of the light used in polymerisation experiments increases nearly proportional to the content of Fe^{3+} ions in TiO_2.

The charge carrier lifetime is shortened due to doping TiO_2 by Fe^{3+} from about 23 ms for the undoped material to 1.5 ms for TiO_2 doped by 3 mol% of Fe^{3+}. So the positive effect by improving the absorption feature is partially compensated by a decreased charge carrier lifetime. The sample containing 1 mol% Fe^{3+} absorbs the light sufficiently and the charge carrier lifetime in the surface region is long enough. So this sample shows the highest activity.

In the concentration range from 3 to 10 mol% of Fe^{3+} the charge carrier lifetime does not depend on the Fe^{3+} content in TiO_2. Nevertheless the photocatalytic activity of the TiO_2 samples decreases down to a completely inactivation with increasing content of Fe^{3+} ions although the light absorption is improved. The crystallites as well as the grain boundary regions in which the Fe^{3+} ions are enriched contribute to the integral light absorption. For Fe^{3+} contents larger than 1 mol% the contribution of iron-rich phases in the grain boundary regions to the integral absorption increases with the Fe^{3+} concentration. From the experimental findings it can be concluded that the grain boundaries in which the Fe^{3+} ions are enriched do not show any photocatalytic activity but act as a light filter and disturb the light absorption by the photocatalytic active TiO_2 crystallites.

The morphology of the samples affects the charge carrier lifetime: in literature [19] is discussed that Fe^{3+} ions on Ti^{4+} lattice places act as recombination centres. The findings presented in this work confirm this. For Fe^{3+} contents above 1 mol% not all Fe^{3+} ions occupy lattices places. In this concentration range a decrease of the anatase primary crystallite size was observed. Consequently in the concentration range above 1 mol% Fe^{3+} the grain boundary area per particle increases with increasing Fe^{3+} content. In the concentration range from 1 to 3 mol% Fe^{3+} a further decrease of the charge carrier lifetime was observed. From this result it can be concluded that grain boundaries within the TiO_2 particles are also effective recombination centres.

All in all the results presented in this work show that only a combination of photocatalytic activity tests, investigations of the photoelectric primary processes in the photocatalyst materials by Photo-EMF measurements and morphology studies can lead to a better understanding of doping effects on the photocatalytic activity.

Acknowledgements

The author is grateful for financial support from the German Research Foundation (DFG). Many thanks to Prof. M. Buchmeiser and Dr. T. Scherzer from the Leibniz Institute for Surface Modification Leipzig (IOM Leipzig) for the opportunity

to perform time resolved IR spectroscopic investigations. Moreover the author acknowledges Prof. G. Israel and Dr. F.W. Müller from the Department of Organic Chemistry at the University of Halle-Wittenberg for the possibility to perform Photo-EMF measurements. Many thanks to Mrs. R. Müller and Mrs. E. Springer, respectively, for doing XRD investigations and specific surface area measurements, respectively.

References

[1] D.A. Tryk, A. Fujishima, K. Honda, Electrochim. Acta 45 (2000) 2363.
[2] A. Fujishima, K. Hashimoto, T. Watanabe, TiO_2 Photocatalysis, Fundamentals and Applications, Bkc Inc., Tokyo, 1999.
[3] N. Serpone, E. Pelizzetti (Eds.), Photocatalysis, Fundamentals and Applications, Wiley, New York, 1989.
[4] D.F. Ollis, H. Al-Ekabi (Eds.), Photocatalytic Purification and Treatment of Water and Air, Elsevier, Amsterdam, 1993.
[5] E. Pelizzetti, M. Schiavello (Eds.), Photochemical Conversion and Storage of Solar Energy, Kluwer Academic Publishers, Dordrecht, 1991.
[6] D.W. Bahnemann, Nachr. Chem. Tech. Lab. 42 (1994) 378.
[7] T. Minabe, D.A. Tryk, P. Sawunyama, Y. Kikuchi, K. Hashimoto, A. Fujishima, J. Photochem. Photobiol. A: Chem. 137 (2000) 53.
[8] M. Grätzel, A. Hagfeldt, Chem. Rev. 95 (1995) 49.
[9] M. Kruggel, G. Israel, J. Inf. Rec. 23 (1–2) (1996) 47.
[10] H. Xu, H. Li, K. Liu, Dyes Pigments 49 (2001) 9.
[11] J. Zhang, D. Wang, Y. Chen, T. Li, H. Mao, H. Tian, Q. Zhou, H. Xu, Thin Solid Films 300 (1997) 208.
[12] Y. Tachibana, I.V. Rubtsov, I. Montanari, K. Yoshihara, D.R. Klug, J.R. Durrant, J. Photochem. Photobiol. A: Chem. 142 (2001) 215.
[13] S. Altobello, C.A. Bignozzi, S. Caramori, G. Larramona, S. Quici, G. Marzanni, R. Lakhmiri, J. Photochem. Photobiol. A: Chem. 166 (2004) 91.
[14] H. Sukihara, S. Sano, T. Yamaguchi, M. Yanagida, T. Sato, Y. Abe, Y. Nagao, H. Arakawa, J. Photochem. Photobiol. A: Chem. 166 (2004) 81.
[15] K.E. Karakitsou, X.E. Verykios, J. Phys. Chem. 97 (1993) 1184.
[16] W. Mu, J.M. Herrmann, P. Pichat, Catal. Lett. 3 (1989) 73.
[17] W. Choi, A. Termin, M.R. Hoffmann, J. Phys. Chem. 98 (1994) 13669.
[18] Y. Yang, X.-J. Li, J.-T. Chen, L.-Y. Wang, J. Photochem. Photobiol. A: Chem. 163 (2004) 517.
[19] C. Paulus, K. Wilke, H.D. Breuer, J. Inf. Rec. 24 (1998) 299.
[20] K. Wilke, H.D. Breuer, J. Photochem. Photobiol. A: Chem. 121 (1999) 49.
[21] K. Rosche, C. Decker, G. Israel, J.-P. Fouassier, Eur. Polym. J. 33 (6) (1997) 849.
[22] A.J. Hoffman, H. Yee, G. Mills, M.R. Hoffmann, J. Phys. Chem. 96 (1992) 5540–5546.
[23] I.R. Bellobono, R. Morelli, C.M. Chiodaroli, J. Photochem. Photobiol. A: Chem. 105 (1997) 89.
[24] I.G. Popovic, L. Katsikas, H. Weller, Pol. Bull. 32 (1994) 597.
[25] Z.Y. Huang, T. Barber, G. Mills, M.-B. Morris, J. Phys. Chem. 98 (1994) 12746.
[26] A.L. Stroyuk, V.M. Granchak, A.V. Korzhak, S.Ya. Kuchmii, J. Photochem. Photobiol. A: Chem. 162 (2004) 339.
[27] F.W. Mueller, C. Damm, G. Israel, J. Inf. Rec. 25 (2000) 533.
[28] G. Israel, F.W. Mueller, C. Damm, J. Harenburg, J. Inf. Rec. 23 (1997) 559.
[29] J.E. Huheey, Inorganic Chemistry, Principles of Structure and Reactivity, Harper & Row, New York, 1983.
[30] C. Damm, D. Völtzke, H.-P. Abicht, G. Israel, J. Photochem. Photobiol. A: Chem. 174 (2005) 171.
[31] A. Merlin, J.P. Fouassier, J. Chim. Phys. 78 (1981) 267.
[32] C. Groenenboom, H.J. Hageman, T. Overeem, A.J.M. Weber, Makromol. Chem. 183 (1982) 281.
[33] T. Scherzer, U. Decker, Nucl. Instrum. Meth. B 151 (1999) 306.
[34] R. Ojah, S.K. Dolui, J. Photochem. Photobiol. A: Chem. 172 (2005) 121.